231656

UCRL-JC-128056
PREPRINT

Thermo-Mechanical Processing and Properties of a Ductile Iron

C. K. Syn
D. R. Lesuer
O. D. Sherby

This paper was prepared for submittal to the
Thermomechanical Processing and
Mechanical Properties of Hypereutectoid Steels
TMS Symposium
Indianapolis, IN
September 15-18, 1997

July 14, 1997

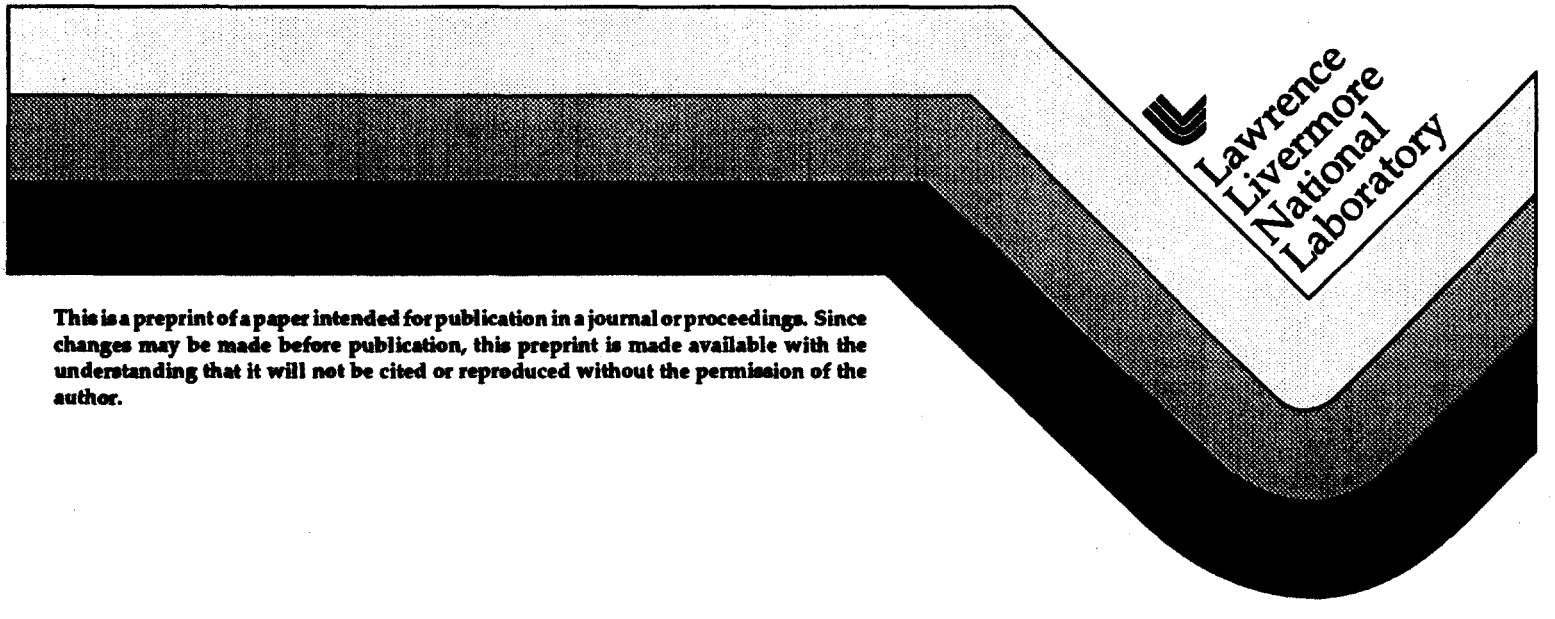

THERMO-MECHANICAL PROCESSING AND PROPERTIES OF A DUCTILE IRON

C. K. Syn*, D. R. Lesuer* and O. D. Sherby**

*Lawrence Livermore national Laboratory, Livermore, CA 94551
**Dep't of Materials Science & Eng., Stanford University, Stanford, CA 94305

Abstract

Thermo-mechanical processing of ductile irons is a potential method for enhancing their mechanical properties. A ductile cast iron containing 3.6% C, 2.6% Si and 0.045% Mg was continuously hot-and-warm rolled or one-step press-forged from a temperature in the austenite range (900°C-1100°C) to a temperature below the A_1 temperature. Various amounts of reduction were used (from 60% to more than 90%) followed by a short heat treatment at 600°C. The heat treatment lead to a structure of fine graphite in a matrix of ferrite and carbides. The hot-and-warm worked materials developed a pearlitic microstructure while the press-forged material developed a spheroidite-like carbide microstructure in the matrix. Cementite-denuded ferrite zones were developed around graphite stringers in the hot-and-warm worked materials, but such zones were absent in the press-forged material. Tensile properties including tensile strength and total elongation were measured along the direction parallel and transverse to the rolling direction and along the direction transverse to the press-forging direction. The tensile ductility and strength both increased with a decrease in the amount of hot-and-warm working. The press-forged materials showed higher strength (645 MPa) than the hot-and-warm worked materials (575 MPa) when compared at the same ductility level (22% elongation).

This work was performed under the auspices of the U.S. Department of Energy by the Lawrence Livermore National Laboratory under Contract No. W-7405-ENG-48.

Introduction

It is the purpose of this paper to discuss some of the mechanical properties of ductile iron after various thermo-mechanical processing steps. Although ductile iron is usually used in the as-cast condition, there is now evidence that such a material can have considerably improved room temperature properties after various hot-and-warm working steps [1-6].

Ductile iron can be classified as a hypereutectoid steel since its typical composition is about 3.5% carbon with about 2.5% silicon. It has many of the characteristics of ultrahigh carbon steels (UHCSs) in that when heated high in the austenite range, it can have as much as 1.6% C in solution. Thus, the transformation products and mechanical processing steps studied extensively in UHCSs[7] can be directly applied to achieving unusual structures and properties in ductile irons. It is the purpose of this paper to show some of the structures and properties obtained in a ductile iron after deformation by hot-and-warm working rolling and by press-forging. Some attention will be paid to the formation of ferrite-free regions during mechanical working, and to relating this structural feature to the diffusion kinetics of carbon and iron in the austenite and ferrite regions.

Iron-Graphite, Iron-Iron carbide Phase Diagram

The selection of appropriate thermo-mechanical working steps requires knowledge of the phases in ductile iron as a function of temperature. Accordingly, Fe-graphite and Fe-Fe_3C phase diagrams for an Fe-2.5% Si-C material are shown in Fig. 1. The phase diagram for Fe-graphite (in dotted lines) is from reference [8], whereas the diagram for Fe-Fe_3C (in solid lines) was constructed by interpolation of the diagrams for the Fe-2% Si-C[9] and Fe-3% Si-C[10] systems.

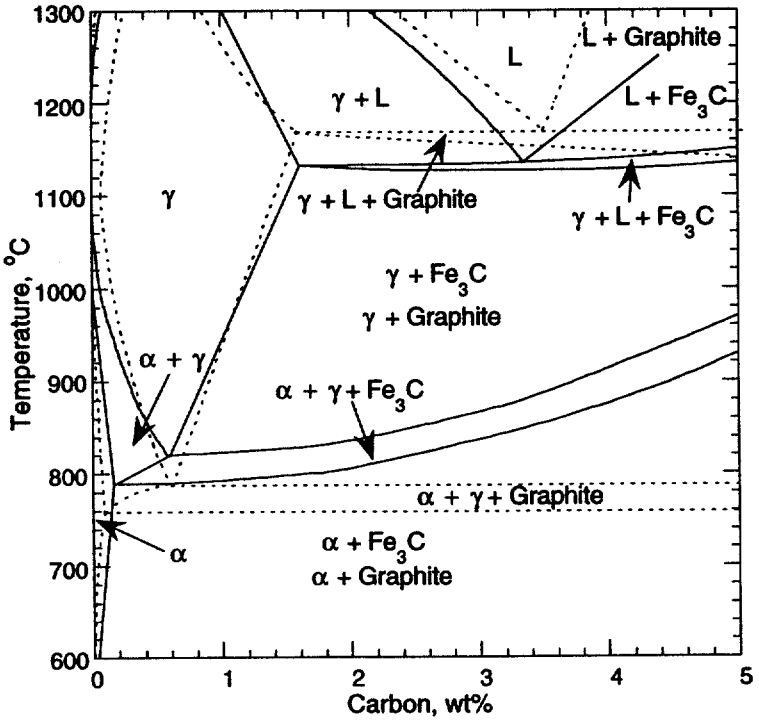

Fig. 1. Estimated phase diagrams for the Fe-Fe_3C (in solid lines) and Fe-graphite (in dotted lines) system containing 2.5% Si.

Several observations that are relevant to the current study can be made from Fig. 1: (1) it defines the amount of C in solution in austenite as a function of temperature (since it is about the same line for both Fe-C and Fe-Fe_3C); (2) it defines the boundary above which the ferrite (α) phase disappears (about 900°C for our 3.5% C ductile iron); (3) it indicates that above 900°C, austenite is likely in metastable equilibrium with graphite and iron carbide just as, at low temperature, ferrite is in metastable equilibrium with iron carbide and graphite; (4) it predicts the melting temperature or start of melting for the ductile iron at about 1120 to 1140°C and indicates the upper limit of metal working; and (5) it suggests that a four phase region likely exists during mechanical working of the ductile iron from the austenite region to the ferrite region, namely ferrite, austenite, graphite and iron carbide.

Material and Experimental Procedures

Material

Ductile iron with a nominal composition of 3.6% C, 2.6% Si, 0.045% Mg and balance Fe was received in the form of rectangular plates with dimensions of 25 mm x 75 mm x 300 mm. Material was obtained in the as-cast and austempered conditions. Small blocks of 25 mm x 32 mm x 38 mm size were sliced from the plates and used as the starting material for thermo-mechanical working.

Processing Procedures

Samples were thermo-mechanically processed using rolling and pressing procedures. Details of the procedures are described elsewhere[6] but can be summarized as follows: Four different processing procedures, involving either hot and warm working (HWW), or multiple warm working, were used: (1) Continuous HWW rolling at 1100 to 800°C in seven passes resulting in a true strain of ε=1.7; (2) Multiple HWW Rolling to get large strains. The sample was deformed to ε=1.2 in six passes at 1100 to 800°C, reheated to 1100°C and deformed to ε=1.45 in two passes with a total ε=2.65; (3) Press-Forging at 1100°C to ε=2.07 in two seconds; (4) Multiple Warm Working Procedure. Samples were heated to 900°C to fully transform ferrite to austenite containing 1.0% carbon, with graphite and probably some undissolved iron carbide. Four rolling steps, with reheating to 900°C, were used. Each rolling step involved four passes with ε=0.12 per pass, resulting in a total deformation of ε=1.80.

The maximum thickness reduction rate (true strain rate) of thickness in each rolling pass was estimated to be about 0.1 sec^{-1}. The forging strain rate was estimated to be about 1 sec^{-1}. All thermo-mechanically worked samples were annealed for 20 minutes at 600°C. The purpose of this treatment was to transform any retained austenite to ferrite plus carbide. The presence of some retained austenite is expected because of ferrite formation during mechanical working and the rejection of carbon into the remaining austenite, making for a high carbon austenite, which remains stable at room temperature.

Tensile Test and Metallography

Tensile test samples with a 5 mm gage width and 12.5 mm gage length were prepared from the rolled or pressed materials by electro-discharge machining (EDM). Samples from the rolled materials were machined in both the longitudinal and transverse directions. For the press-forged materials, tensile samples were machined with the tensile axis parallel to the radial direction. All tensile tests were performed at room temperature. Optical and scanning electron microscopy of as-received and thermo-mechanically processed and heat treated materials were performed.

Results and Discussion

Microstructure

Typical optical microstructures of the as-cast and as-austempered materials in the as-received condition are shown in Figs. 2(a) and (b). Examples of microstructures obtained after continuous HWW and press-forging of the as-cast material followed by the short annealing treatment are shown in Figs. 3(a) and (b), respectively. Mechanical working (and annealing)

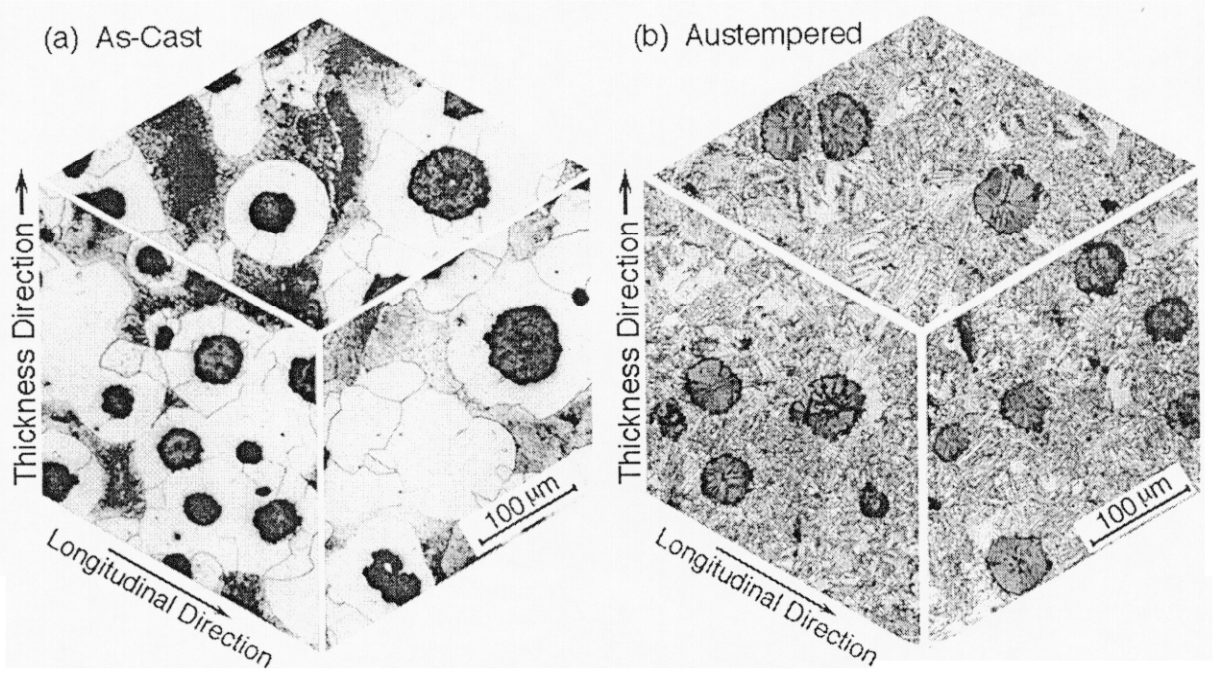

Fig. 2. Optical microstructures of the (a) as-cast and (b) as-austempered materials in the as-received condition.

leads to the following general microstructural features: (1) highly elongated graphite nodular particles, increasing in aspect ratio with increasing mechanical working (Fig. 3(a)) with the exception of the press-forged sample (Fig. 3(b)); (2) cementite-denuded ferrite zones are evident, usually located adjacent to the graphite stringers in the HWW treated material, but not in the press-forged one; (3) the dark appearing regions seen in the micrographs of Figs. 3(a) and (b) (that are not graphite nodules) are regions containing ferrite and cementite as shown in the corresponding high magnification scanning electron micrographs Figs. 4(a) and (b). The HWW sample shows a microstructure consisted of fine pealite colonies (Fig. 4(a)). The press-forged material (Fig. 4(b)) shows a spheroidized carbide structure expected from an uphill transformation of retained austenite as described elsewhere[6]. The retained austenite resulted from the rapid cooling from 1100°C during press forging.

Tensile Properties

The tensile strengths and tensile ductilities of the mechanically processed ductile iron are shown in Fig. 5 plotted as a function of the degree of mechanical work, $\varepsilon_w = -\ln (h_o/h_f)$, where h_o is the initial thickness and h_f is the final thickness. As can be seen, there is a strong effect of the

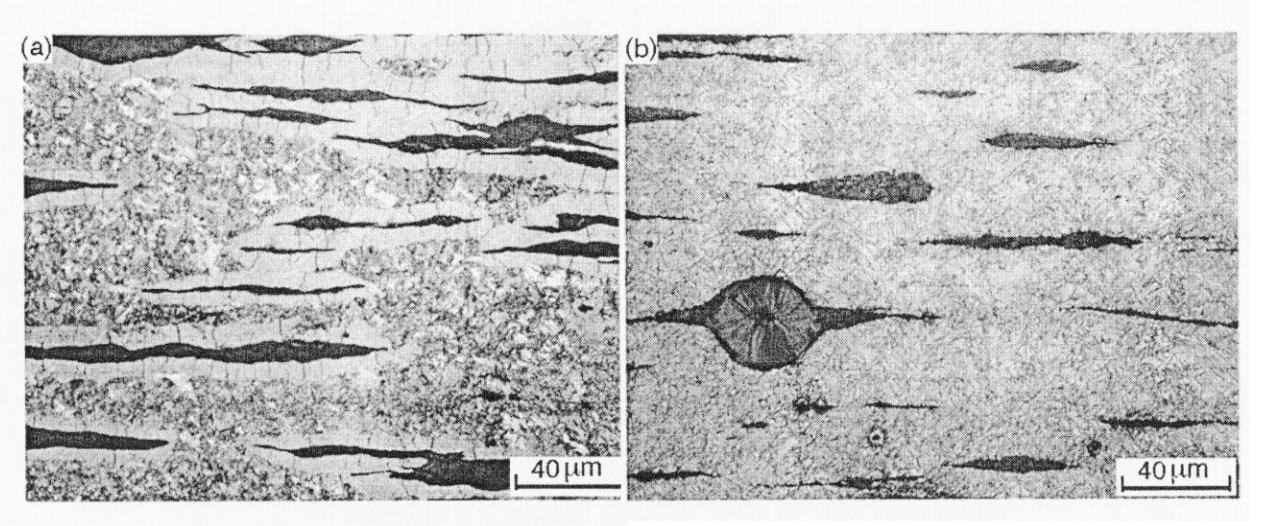

Fig. 3. Optical microstructures obtained after (a) continuous HWW and (b) press-forging of the as-cast material and the short annealing treatment.

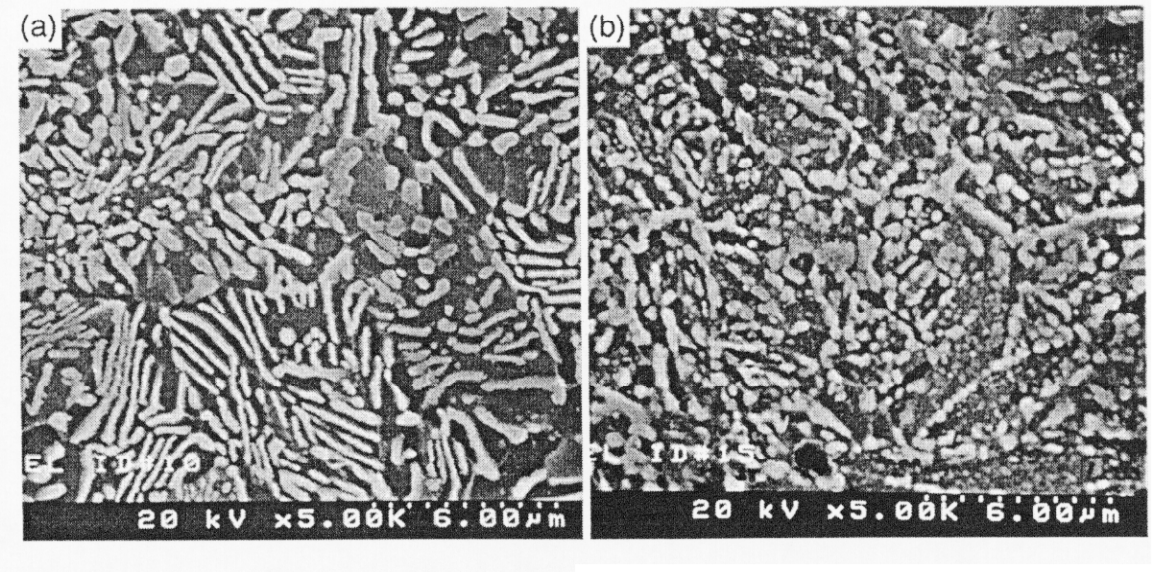

Fig. 4. SEM photomicrographs (a) and (b) of the dark appearing regions in the micrographs of Figs. 3(a) and (b) (that are not graphite nodules), respectively.

processing route and the amount of deformation during processing on the strength and ductility. Both the strength and the tensile ductility are seen to decrease with an increase in the amount of work. This correlation between strength and ductility is different from that typically observed in ductile irons in which the tensile ductility decreases as the strength is increased[11]. The basis of the unexpected result obtained here can be understood in terms of the materials resistance to failure. If failure is delayed, the strain to fracture will be higher and, therefore, a higher fracture strength will result. This concept can be tested with the microstructure-and-property results obtained here and has been discussed elsewhere[6].

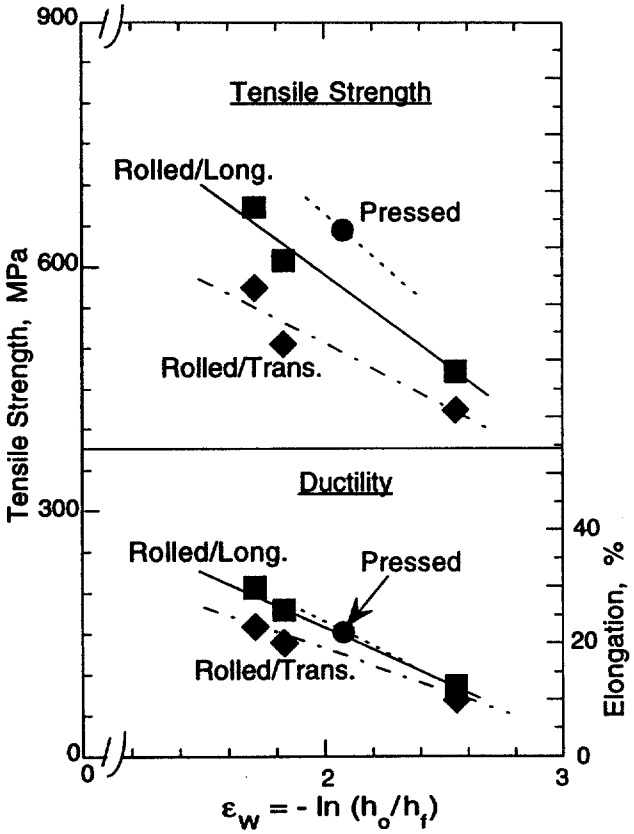

Fig. 5. Tensile strength and ductility vs. working strain for ductile iron.

In Fig. 5, the longitudinal samples show both a higher strength and higher ductility than the transverse samples. This result is readily explained by the morphology of the graphite relative to the test direction. In the transverse sample, the cross-sectional area of the graphite normal to the tensile axis is larger than the cross-sectional area of graphite in the longitudinal sample. The larger cross-sectional area of graphite in the transverse sample produces higher local stresses in the matrix surrounding a cracked graphite ribbon than in the longitudinal sample. Thus, damage development and failure will occur at lower stress, leading to lower ductility and lower strength values in the transverse sample. Another variable to consider is texture development during rolling. No studies on texture, however, have been done on the rolled ductile iron and therefore this variable remains to be explored.

The press-forged ductile iron shows the highest tensile strength when compared at the same mechanical working strain, see Fig. 5. The tensile strength and total elongation data from Fig. 5 for the different processing conditions were replotted in Fig. 6. The press forged material also shows the highest tensile strength when compared at the same elongation or ductility level as seen in Fig. 6. The higher strength results from the smaller nodule sizes that are observed in the press-forged material relative to the rolled materials. Smaller graphite nodules are obtained because of carbon dissolution at the temperature of pressing (1100°C) and subsequent rapid pressing. Since the sample was rapidly cooled during pressing, a higher concentration of carbon was retained in austenite during cooling than in the rolled material. The dissolved carbon became iron carbide during the heat treating step at 600°C and did not increase the volume fraction of graphite. Another reason for the higher strength is the absence of a cementite denuded ferrite zone around graphite stringers in the press-forged material as shown in Fig. 3(b). The spheroidized carbide structure developed right around the graphite stringers is inherently stronger than the cementite-denuded carbon-free

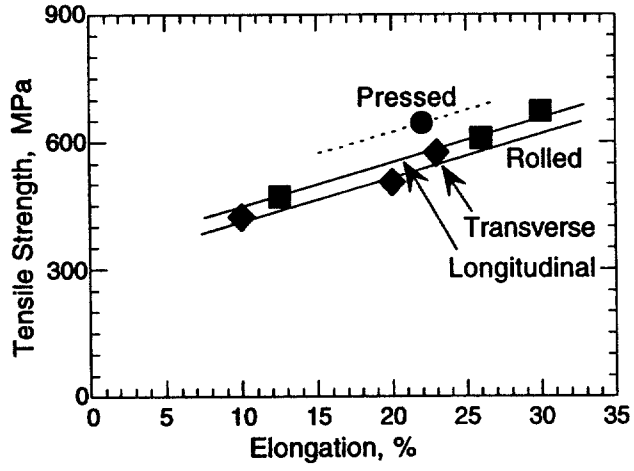

Fig. 6. Tensile strength vs. elongation for press-forged ductile iron studied.

ferrite zones present in the rolled materials.

Extrapolation of the data given in Fig. 5 to lower working strains suggests an interesting trend in strength and ductility at strains below 1.7 as shown in Fig. 7. It seems reasonable that the trend of increasing strength and ductility with decreasing working strain may reach a maximum and then decrease to the levels of as-cast strength and ductility. Further study is warranted to develop a processing condition which will give an optimal strength and ductility at a lower strain level than used in the present study.

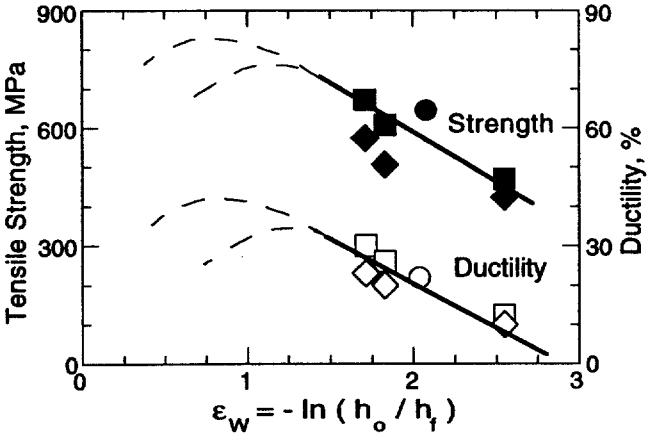

Fig. 7. Extrapolation of the data given Fig. 5 to low working strain.

Cementite Denuded Zones

The absence of cementite-denuded zones in the press-forged material (Fig. 3(b)) and their presence in the HWW (Fig. 3(a)) material can be explained qualitatively from the phase diagram shown in Fig. 1. The materials were initially heated to 1100°C and the structure consisted of austenite, cementite and graphite, as can be seen from the phase diagram. During the thermo-mechanical processing, as each material cools down from 1100°C, carbon in the austenite either migrates to the nearest graphite nodules or forms more cementite (proeutectoid carbide) particles. However, the large deformation during the thermo-mechanical processing would prevent the cementite formation and even enhance the dissolution of the existing cementite particles by providing fast diffusion paths resulting from dislocation production. Since graphite is thermodynamically more stable than cementite, deformation at elevated temperature, and slow cooling will always promote dissolution of cementite particles. In the present case of the HWW material, the slow plastic deformation combined with slow cooling lead to the creation of the denuded zones around graphite nodules. On the other hand, the fast deformation and rapid cooling of the press forged material prevented the cementite particles from dissolving. The rapid cooling also prevented the austenite-to-ferrite transformation and lead to a large volume fraction of retained austenite or martensite in the as-forged condition, which in turn transformed to fine spheroidized carbide structure during post heat treatment as shown in Fig. 3(b).

The kinetics of denuded zone formation can be understood in terms of the dissolution mechanisms of carbon and iron during the thermo-mechanical processing. The dissolution process is controlled by the slower of the two diffusing species, iron and carbon. The average width, λ, of the denuded zones in Fig. 3(a) was estimated to be about 6 μm and the total deformation time, t, during the HWW processing was about 20 seconds. Thus the diffusivity, D, required for rate-controlling species to move a distance of 6 μm was estimated to be about $4.5 \cdot 10^{-13}$ m^2/sec. from the simple relationship, $\lambda = 2 \cdot (D \cdot t)^{1/2}$. This calculated value of diffusivity was compared with the known diffusivity data for carbon and iron in ferrite or austenite for the temperature range of thermo-mechanical processing used in the present study as shown in Fig. 8. Diffusivity data in Fig. 8 were calculated from the pre-exponential factors and activation energies cited in reference 12. A horizontal line representing the calculated diffusivity $4.5 \cdot 10^{-13}$ m^2/sec. was drawn in Fig. 8. One can see that the carbon diffusivity is more than an order of magnitude higher than this value over the temperature range of the thermo-mechanical processing, and hence it cannot be the rate-controlling mechanism. The carbon, once dissolved, diffuses rapidly to the graphite boundary. Therefore, since iron moves slower than carbon, it must be the iron diffusivity that controls the dissolution rate of cementite particles. The calculated diffusivity is,

however, much higher than the diffusivity of iron-in-austenite and iron-in-ferrite. Thus, it must be a strain-enhanced iron diffusion that is taking place, either by creation of numerous dislocation-short-circuit contribution or generation of vacancies[13]. The denuding process must be occurring in the temperature range of 750°C to 950°C where lots of iron carbide precipitates will be present as can be inferred from the phase diagram in Fig. 1.

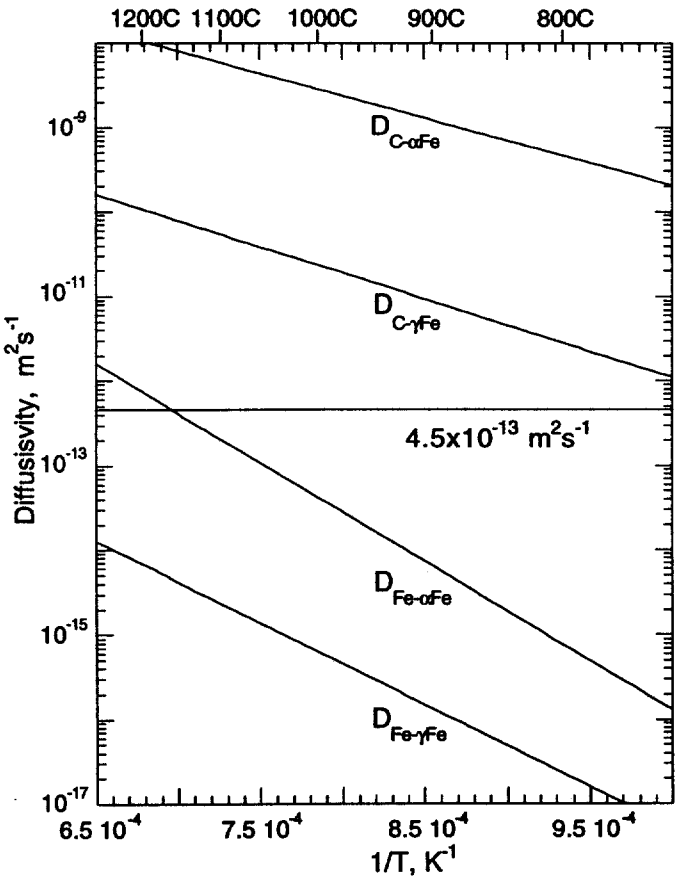

Fig. 8. Diffusivity of iron and carbon in ferrite and austenite irons estimated from data in reference 12.

Conclusions

1. A ductile cast iron has been shown to be readily thermo-mechanically worked by continuous hot-and-warm rolling and by one-step large strain press-forging.

2. In the strain range studied (ε_w=1.7 to 2.5), tensile strength and ductility both increase with a decrease in the amount of hot and warm working.

3. The press-forged ductile iron showed higher strength than the rolled ductile iron when compared at the same strain.

4. Cementite denuded ferrite zones around graphite stringers are formed in the continuos hot-and-warm worked condition but not in the press-forged condition.

5. The formation of denuded zones are rate-controlled by iron diffusion in iron during the thermo-mechanical processing procedures.

Acknowledgment

The authors are gratefully to Dr. P. H. Mani, Technical Director, Wagner Castings Co., Decatur, Illinois, for providing ductile cast iron materials in as-cast and austempered conditions. The authors thank Jim Mathews for help in metal working, Bob Accardo for heat treating, Jeffery Groth for sample machining, George Yanes and Reynold Lum for tensile testing, and Jim Ferreira and Ed Sedillo for optical and SEM metallography. This work was performed under the auspices of the U.S. Department of Energy by the Lawrence Livermore National Laboratory under contract No. W-7405-ENG-48.

References

1. A. Matsushita, W. Yamamoto, K. Hosoo and K. Ikawa, *Proc. 93rd Meeting of the Japan Foundrymen's Society*, 1978, The Japan Foundrymen's Society, Tokyo, Japan, p.13 (in Japanese).
2. A. Kagawa, T. Okamoto, H. Matsumoto, and K. Kamei, *Journal of the Japan Foundrymen's Society*, 1983, vol. 55 (10), pp. 597-602 (in Japanese).
3. D. J. Moore, T. N. Rouns and K. B. Rundman, *J. Heat Treating*, 1985, vol. 4(1), pp. 7-24.
4. K. Nagai and K. Kishitake, *J. Japan Foundrymen's Society*, 1990, vol. 62(5), pp. 338-343 (in Japanese).
5. S. Yamada and T. Kobayashi, *J. Japan Foundrymen's Society*, 1995, vol. 67 (6), pp. 385-390 (in Japanese).
6. C. K. Syn, D. R. Lesuer and O. D. Sherby, Metall. Mater. Trans. A, 1997, vol. 28A (5), pp. 1213-1218.
7. D. R. Lesuer, C. K. Syn, A. Goldberg, J. Wadsworth and O. D. Sherby, JOM, 1993, vol. 45 (8), pp. 40-46.
8. D. B. Craig, M. J. Hornung and T. K. McCluhan, "Gray Cast Iron", from Casting, vol. 15, p. 629, *Metals Handbook 9th Edition, ASM*, 1988.
9. From Fig. 1 of "Basic Metallurgy of Cast Irons", in Vol. 1, Properties and Selection: Irons and Steels, *Metals Handbook, 9th Edition, ASM*, 1977.
10. O. D. Sherby and T. Oyama, *U.S. Patent* No. 4,533,390, Aug. 6, 1985.
11. I. C. H. Hughes, "Ductile Iron", in Casting, Vol. 15, pp. 647-665, *Metals Handbook, 9th Edition, ASM* 1988.
12. Y. Adda and J. Philibert, *La Diffusion dans les Solides*, vol. 2, Institut National des Sciences et Techniques Nucléaires, Saclay, & Presses Universitaires de France, Paris, France, 1966.
13. M. J. Harrigan and O. D. Sherby, Mater. Sci. Eng., 1971, vol. 7, pp. 177-189.

Technical Information Department • **Lawrence Livermore National Laboratory**
University of California • Livermore, California 94551